

# Deconfinement phase transition and the quark condensate

Christian S. Fischer<sup>1,2</sup>

<sup>1</sup>*Institut für Kernphysik, Technische Universität Darmstadt, Schlossgartenstraße 9,  
D-64289 Darmstadt, Germany*

<sup>2</sup>*GSI Helmholtzzentrum für Schwerionenforschung GmbH, Planckstr. 1 D-64291 Darmstadt, Germany.*  
(Dated: February 18, 2019)

We study the dual quark condensate as a signal for the deconfinement phase transition. This order parameter for center symmetry has been defined recently by Bilgici et al. within lattice QCD. In this work we determine the dual condensate with functional methods using a formulation of the Dyson-Schwinger equations for the Landau gauge quark propagator on a torus. We study the chiral and deconfinement phase transitions of quenched QCD by related susceptibilities. The gauge fixed functional formalism yields similar results for the deconfinement transition as lattice QCD.

PACS numbers: 12.38.Aw, 12.38.Lg, 11.10.Wx

## Introduction

The chiral and deconfinement transition of QCD is a subject of continuous interest. One of the unsolved problems in this respect is the question of an underlying mechanism relating both phenomena. Strictly speaking chiral and deconfinement phase transitions occur in opposite sectors of the theory. The chiral condensate acts as order parameter for the chiral phase transition in the chiral limit  $m = 0$ , whereas the Polyakov loop signals center symmetry breaking at the deconfinement transition for infinitely heavy quark masses. At intermediate masses both transitions develop a fascinating interplay which is not yet understood in detail. This interplay needs to be explored by nonperturbative tools such as lattice gauge theory and functional methods.

Functional methods allow to relate both transitions to the behaviour of correlation functions and the details of the quark-gluon interaction. This sheds light on potential connections between dynamical chiral symmetry breaking and confinement. Whereas at zero temperature the long range behaviour of correlations may be relevant [1], it is the mid-momentum modes which are pertinent for the deconfinement phase transition [2].

Order parameters for deconfinement are not easily accessible by functional methods. In Ref. [2] a method has been developed to determine the Polyakov loop potential, whereas in Ref. [3] the analytic structure of the quark propagator has been studied. In this letter we report on a calculation of the dual quark condensate or 'dressed Polyakov loop' with functional methods.

This order parameter for center symmetry has emerged from a series of works connecting spectral sums of the Dirac propagator with Polyakov loops and their correlators. Initiated by a work of Gattringer [4] these ideas have been extended and refined in Ref. [5, 6]. Within the framework of lattice gauge theory the dual condensate  $\Sigma_n$  has been introduced in Ref. [7]. It is defined by the Fourier-transform

$$\Sigma_n = - \int_0^{2\pi} \frac{d\varphi}{2\pi} e^{-i\varphi n} \langle \bar{\psi}\psi \rangle_\varphi \quad (1)$$

of the ordinary quark condensate evaluated with respect to  $U(1)$ -valued boundary conditions with a phase  $e^{i\varphi}$  in the temporal direction of the Euclidean theory. For the usual antiperiodic boundary conditions for fermions we have  $\varphi = \pi$ , whereas  $\varphi = 0$  corresponds to periodic boundary conditions. The  $\varphi$ -dependent quark condensate  $\langle \bar{\psi}\psi \rangle_\varphi$  is proportional to a sum over closed loops winding  $n$ -times around the compact time direction:

$$\langle \bar{\psi}\psi \rangle_\varphi = \sum_{l \in \mathcal{L}} \frac{e^{i\varphi q(l)}}{m^{|l|}} U(l). \quad (2)$$

Here  $\mathcal{L}$  denotes the set of all closed loops  $l$  with length  $|l|$  on a lattice and  $m$  is the quark mass.  $U(l)$  stands for the chain of link variables in a loop  $l$  multiplied with appropriate sign and normalisation factors, see Ref. [7] for details. Each loop that closes around the temporal boundary picks up factors of  $e^{\pm i\varphi}$  according to its winding number  $q(l)$ . The Fourier transform in (1) projects out those loops with winding number  $n$ . The dual condensate  $\Sigma_1$  then corresponds to loops that wind exactly once and is called the 'dressed Polyakov loop' [7]. This quantity transforms under center transformation identically as the conventional Polyakov loop [8] and is therefore an order parameter for center symmetry. The numerical agreement between dressed and conventional Polyakov loop has been established for gauge groups  $SU(3)$  [9] and, remarkably, also for the centerless  $G(2)$  [10].

In this letter we determine the dual quark condensate with functional methods. As a tool we employ the Dyson-Schwinger equations of Landau gauge QCD at finite temperature (see e.g. [11, 12]) formulated on a torus. However, we wish to emphasize that the method is sufficiently general to be of equal use in other functional approaches as e.g. the functional renormalisation group (see e.g. [13]). We evaluate the conventional and the dual quark condensate, Eq. (1), from the trace of the quark propagator as a function of temperature. The corresponding susceptibility allows to locate the deconfinement transition. We thus demonstrate that functional methods in the gauge fixed theory are capable to produce similar results as (non-gauge fixed) lattice simulations.

### Dyson-Schwinger equations on a torus

In the following we work in Euclidean space with compact time and space directions and box size  $V = L^3 \times 1/T$  with temperature  $T$  and  $1/T \ll L$ . In coordinate space we choose periodic boundary conditions in the three spatial directions for the quark and gluon fields. The gluon field also obeys periodic boundary conditions in the temporal direction. For the fermion field  $\psi$  we use the generalised,  $U(1)$ -valued boundary conditions  $\psi(\vec{x}, 1/T) = e^{i\varphi} \psi(\vec{x}, 0)$  in the temporal direction as described above. In loop integrals in momentum space this results in Matsubara modes  $\omega_p(n_t) = (2\pi T)(n_t + \varphi/2\pi)$  in the  $p_4$ -direction,

which depend on the boundary angle  $\varphi \in [0, 2\pi[$ . In the spatial directions we have the usual Matsubara sums which are treated with the techniques described in [14].

In Euclidean momentum space at nonzero temperature the renormalised dressed quark propagator is given by

$$S(\vec{p}, \omega_p) = [i\gamma_4 \omega_p C(\vec{p}, \omega_p) + i\gamma_i p_i A(\vec{p}, \omega_p) + B(\vec{p}, \omega_p)]^{-1}, \quad (3)$$

with vector and scalar quark dressing functions  $C, A, B$ , cf. Ref. [11]. These can be calculated from the corresponding Dyson-Schwinger equation shown diagrammatically in Fig. 1. It reads

$$S^{-1}(\vec{p}, \omega_p) = Z_2 S_0^{-1}(\vec{p}, \omega_p) - C_F \frac{Z_2}{\tilde{Z}_3} \frac{g^2 T}{L^3} \sum_{n_t, n_i} \gamma_\mu S(\vec{k}, \omega_k) \Gamma_\nu(\vec{k}, \omega_k, \vec{p}, \omega_p) D_{\mu\nu}(\vec{p} - \vec{k}, \omega_p - \omega_k). \quad (4)$$

where the sum is over temporal and spatial Matsubara modes. The Casimir  $C_F = (N_c^2 - 1)/N_c$  stems from the colour trace; in this work we only consider the gauge group  $SU(2)$ . Furthermore,  $D_{\mu\nu}$  denotes the gluon propagator in Landau gauge and  $\Gamma_\nu$  the (reduced) quark-gluon vertex. The bare quark propagator  $S_0$  is given by (3) with  $A = C = 1$  and  $B = Z_m m$ , where  $m$  is the bare quark mass. The renormalisation factors  $Z_2$ ,  $Z_m$  and  $\tilde{Z}_3$  are determined in the renormalisation process.

In order to solve this equation we have to specify explicit expressions for the gluon propagator and the quark-gluon vertex. For the momentum range relevant for Eq. (4) we nowadays have very accurate solutions for the gluon propagator at zero temperature from both, lattice calculations and functional methods, see e.g. [15] and references therein. The temperature dependence of the gluon propagator, however, is much less explored. In [16] a combined study on the lattice and from Dyson-Schwinger equations records a very different temperature dependence of the electric and magnetic sector. Whereas the magnetic part of the propagator seems to be indifferent to the deconfinement phase transition, the electric part is strongly increased at and around the critical temperature  $T_c \approx 300$  MeV. Although the lattice data still have considerable systematic errors they may correctly represent the qualitative temperature dependence of the gluon propagator. We therefore use a temperature de-

pendent fit to the data as input into the DSE. The gluon propagator is then given by

$$D_{\mu\nu}(q) = \frac{Z_T(q)}{q^2} P_{\mu\nu}^T(q) + \frac{Z_L(q)}{q^2} P_{\mu\nu}^L(q) \quad (5)$$

with  $q = (\vec{q}, \omega_q)$  and dressing functions  $Z_T(\vec{q}, \omega_q)$  and  $Z_L(\vec{q}, \omega_q)$ . The transverse and longitudinal projectors with respect to the heat bath are given by

$$\begin{aligned} P_{\mu\nu}^T(q) &= \left( \delta_{ij} - \frac{q_i q_j}{q^2} \right) \delta_{i\mu} \delta_{j\nu}, \\ P_{\mu\nu}^L(q) &= P_{\mu\nu}(q) - P_{\mu\nu}^T(q), \end{aligned} \quad (6)$$

with  $(i, j = 1 \dots 3)$ . The  $SU(2)$  lattice results of Ref. [16] are well fitted by

$$\begin{aligned} Z_{T,L}(\vec{q}, \omega_q, T) &= \frac{q^2 \Lambda^2}{(q^2 + \Lambda^2)^2} \left\{ \left( \frac{c}{q^2 + \Lambda^2 a_{T,L}(T)} \right)^2 \right. \\ &\quad \left. + \frac{q^2}{\Lambda^2} \left( \frac{\beta_0 \alpha(\mu) \ln[q^2/\Lambda^2 + 1]}{4\pi} \right)^\gamma \right\} \end{aligned} \quad (7)$$

with the temperature independent scale  $\Lambda = 1.4$  GeV and the coefficient  $c = 9.8$  GeV<sup>2</sup>. For gauge group  $SU(2)$  we have  $\beta_0 = 22/3$  and  $\gamma = -13/22$  in the quenched theory and we renormalise at  $\alpha(\mu) = 0.3$ . The temperature dependent scale modification parameters  $a_{T,L}(T)$  are given in table I. In order to extend this fit to temperatures not given in the table we assume  $a_{T,L}(T)$  to be temperature independent below  $T = 119$  MeV and only slowly rising

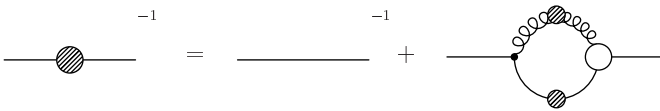


FIG. 1: The Dyson-Schwinger equation for the quark propagator. Filled circles denote dressed propagators whereas the empty circle stands for the dressed quark-gluon vertex.

T[MeV]	0	119	298	597
$a_T(T)$	1	1	1.34	1.65
$a_L(L)$	1	1	0.8	4.0

TABLE I: Temperature dependent fit parameter of Eq.(7).

above  $T = 597$  MeV. For  $T \in [119, 597]$  MeV we use cubic splines to interpolate smoothly between the values given in table I. We expect the systematic error of this procedure to be of the same order as the systematic errors inherent in the lattice data. Naturally, by this procedure we also take over the scale determined on the

lattice calculations using the string tension  $\sqrt{\sigma} = 0.44$  GeV [16].

For the quark-gluon vertex with gluon momentum  $q = (\vec{q}, \omega_q)$  and the quark momenta  $p = (\vec{p}, \omega_p), k = (\vec{k}, \omega_k)$  we employ the following temperature dependent model

$$\Gamma_\nu(q, k, p) = \tilde{Z}_3 \left( \delta_{4\nu} \gamma_4 \frac{C(k) + C(p)}{2} + \delta_{j\nu} \gamma_j \frac{A(k) + A(p)}{2} \right) \left( \frac{d_1}{d_2 + q^2} + \frac{q^2}{\Lambda^2 + q^2} \left( \frac{\beta_0 \alpha(\mu) \ln[q^2/\Lambda^2 + 1]}{4\pi} \right)^{2\delta} \right). \quad (8)$$

where  $\delta = -9/44$  is the anomalous dimension of the vertex. Note that because of  $\gamma + 2\delta = -1$  the gluon dressing function together with the quark-gluon vertex behave like a running coupling at large momenta; this is a necessary boundary condition for any model interaction in the quark DSE. The dependence of the vertex on the quark dressing functions  $A$  and  $C$  is dictated by the Slavnov-Taylor identity. The remaining fit function is purely phenomenological, see e.g. [17] where an elaborate version of such an ansatz has been used to describe meson observables. Here we use  $d_1 = 7.6 \text{ GeV}^2$  and  $d_2 = 0.5 \text{ GeV}^2$ . We also used a range of alternative ansätze to explore whether the qualitative results of this work are independent of the details of the ansatz; this is indeed the case. Perhaps of particular interest is the fact that the confinement-deconfinement phase transition is insensitive to the deep infrared behaviour of the gluon propagator and the quark-gluon vertex, i.e. to the question of scaling vs. decoupling in the sense specified in [15]. Details will be reported elsewhere.

The quark-DSE is solved numerically using the input specified above, the three-volume  $V = (5 \text{ fm})^3$  and  $n_t = 8$  Matsubara frequencies in the temporal direction. The renormalisation conditions are  $C(\mu) = 1$  and  $B(\mu) = m$  with  $\mu = (\vec{\mu}, \pi T)$  and  $\vec{\mu}^2 = 20 \text{ GeV}^2$ . The resulting quark dressing functions are subsequently used to determine the quark condensate according to

$$\langle \bar{\psi} \psi \rangle_\varphi = \frac{4Z_2 N_c T}{L^3} \sum_{n_t, n_i} \frac{B(\vec{p}, \omega_p(\varphi))}{\omega_p^2(\varphi) C^2 + \vec{p}^2 A^2 + B^2}, \quad (9)$$

where we indicated the dependence of the frequencies on the generalised  $U(1)$ -boundary conditions. For nonvanishing bare quark masses  $m$  this expression is divergent and, at least in the continuum limit, has to be renormalised accordingly. For the purpose of this letter, however, it is sufficient to work with the regularised expression at fixed ultraviolet cut-off corresponding to fixed lattice spacing.

### Numerical results

First we explore the dependence of the quark condensate on the boundary angle  $\varphi$  which can be read off Eq. (2). Each loop winding  $n$  times around the temporal direction

of the torus contributes a factor  $\cos(n\varphi)$ . Consequently the integrand in Eq. (1) can be expanded as a series in  $\cos(n\varphi)$  and is symmetric in the interval  $[0, 2\pi]$ . This behaviour is clearly seen also in our numerical result for  $\Delta(\varphi) \equiv \langle \bar{\psi} \psi \rangle_\varphi$  shown in Fig. 2. For  $T = 200$  MeV far below the deconfinement transition we find almost no angular dependence of the condensate. This is especially true for the heavier quark mass  $m = 60$  MeV. For  $T = 400$  MeV far above the transition the behaviour is markedly different and we observe the characteristic cosine-type of behaviour of the condensate that we expect from Eq. (2). This is in nice agreement with the results of Ref. [7] on the lattice. The angular dependence of the condensate can be fitted well by  $\Delta(\varphi) = \sum_{n=0}^N a_n \cos(n\varphi)$ . Whereas for the heavier mass  $m = 60$  MeV one obtains an excellent fit with  $N = 3$ , at least  $N = 7$  is needed for the smaller mass  $m = 10$  MeV. Thus the closer one gets to the chiral limit the more contributions from Polyakov loops with higher winding number around the temporal direction are significant. This is a direct consequence of the mass factor  $1/m^{|l|}$  in the expansion Eq. (2) and also seen on the lattice [18].

By far the largest contribution to the angular depen-

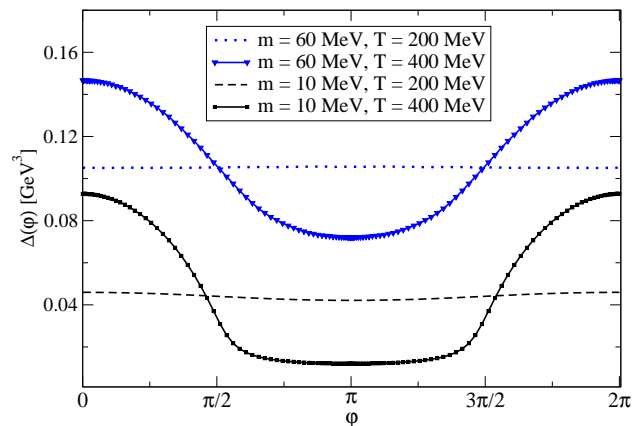


FIG. 2: The angular dependence of the quark condensate  $\Delta(\varphi) \equiv \langle \bar{\psi} \psi \rangle_\varphi$  below and above the deconfinement transition for two different quark masses.

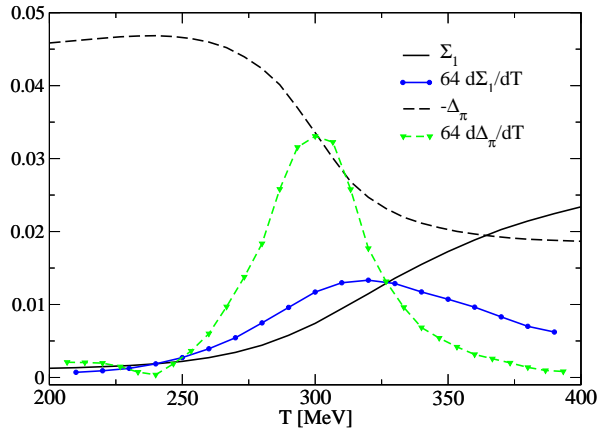


FIG. 3: The temperature dependence of the dressed Polyakov-loop  $\Sigma_1$  and the conventional quark condensate  $\Delta_\pi \equiv \langle \bar{\psi}\psi \rangle_{\varphi=\pi}$  together with their derivatives for  $m = 10$  MeV.

dence of the condensate comes from loops with  $n = 1$  which are projected out by the Fourier transformation (1) to the dual condensate. The resulting temperature dependence of the dressed Polyakov loop is shown in Fig. 3 together with the conventional quark condensate and their derivatives. One clearly observes a change of behaviour in both, the conventional and the dual condensate above  $T = 270$  MeV. The temperature derivative of both quantities has a peak in the region  $T_c = 300 - 320$  MeV signalling the chiral and deconfinement transition. Note that although both transitions are calculated from quantities with direct relation to the spectral properties of the quark propagator they do not necessarily give the same transition temperatures. On the contrary, the chiral transition occurs about 10–20 MeV below the deconfinement transition. Whether the quantitative aspects of

this difference is a model-independent result has to be investigated in more detail.

Finally we wish to point out that the absolute magnitude of our dressed Polyakov loop is about a factor of five smaller than the one calculated on the lattice [7]. This difference may be attributed to different current quark masses, a difference in the gauge group considered ( $SU(2)$  vs.  $SU(3)$ ) and/or may be a renormalisation issue. This has to be clarified in future work.

### Concluding remarks

In this letter we have determined the dual condensate or dressed Polyakov loop by solving the Dyson-Schwinger equations for the quark propagator on a compact manifold. This order parameter for center symmetry measures contributions from closed loops winding once around the time direction. We observe a significant rise of the dressed Polyakov loop around and above the deconfinement transition temperature together with a significant decrease of the ordinary quark condensate. The angular dependence of the quark condensate shows a characteristic dependence of the quark mass: the lighter the quark the more contributions arise from loops with winding numbers larger than one. An obvious next step is to investigate what happens to the transition temperatures when the backreaction of the quarks onto the Yang-Mills sector is included. Particularly interesting in this respect is the case  $N_f = 2 + 1$  which recently is a subject of intense debate [19, 20] in the lattice community.

### Acknowledgments

I thank Falk Bruckmann, Christof Gattringer, Jens Müller and Jan Pawłowski for discussions. I am grateful to Axel Maas for discussions and for making the lattice data of Ref. [16] available. This work has been supported by the Helmholtz Young Investigator Grant VH-NG-332 and by the Helmholtz Alliance HA216-TUD/EMMI.

- 
- [1] R. Alkofer, C. S. Fischer, F. J. Llanes-Estrada and K. Schwenzer, *Annals Phys.* **324** (2009) 106.
  - [2] J. Braun, H. Gies and J. M. Pawłowski, arXiv:0708.2413 [hep-th]; F. Marhauser and J. M. Pawłowski, arXiv:0812.1144 [hep-ph].
  - [3] A. Bender, D. Blaschke, Y. Kalinovsky and C. D. Roberts, *Phys. Rev. Lett.* **77** (1996) 3724.
  - [4] C. Gattringer, *Phys. Rev. Lett.* **97** (2006) 032003.
  - [5] F. Bruckmann, C. Gattringer and C. Hagen, *Phys. Lett. B* **647** (2007) 56.
  - [6] F. Synatschke, A. Wipf and C. Wozar, *Phys. Rev. D* **75** (2007) 114003; F. Synatschke, A. Wipf and K. Langfeld, *Phys. Rev. D* **77** (2008) 114018.
  - [7] E. Bilgici, F. Bruckmann, C. Gattringer and C. Hagen, *Phys. Rev. D* **77** (2008) 094007.
  - [8] A. M. Polyakov, *Phys. Lett. B* **72** (1978) 477; L. Susskind, *Phys. Rev. D* **20**, 2610 (1979).
  - [9] F. Bruckmann, C. Hagen, E. Bilgici and C. Gattringer, *PoS LATTICE2008* (2008) 262.
  - [10] J. Danzer, C. Gattringer and A. Maas, *JHEP* **0901** (2009) 024.
  - [11] C. D. Roberts and S. M. Schmidt, *Prog. Part. Nucl. Phys.* **45**, S1 (2000);
  - [12] A. Maas, J. Wambach and R. Alkofer, *Eur. Phys. J. C* **42** (2005) 93.
  - [13] J. Braun and H. Gies, *JHEP* **0606** (2006) 024.
  - [14] C. S. Fischer, R. Alkofer and H. Reinhardt, *Phys. Rev. D* **65** (2002) 094008; C. S. Fischer and M. R. Pennington, *Phys. Rev. D* **73** (2006) 034029; C. S. Fischer, A. Maas, J. M. Pawłowski and L. von Smekal, *Annals Phys.* **322** (2007) 2916.
  - [15] C. S. Fischer, A. Maas and J. M. Pawłowski, arXiv:0810.1987 [hep-ph].
  - [16] A. Cucchieri, A. Maas and T. Mendes, *Phys. Rev. D* **75**, 076003 (2007).
  - [17] C. S. Fischer and R. Williams, *Phys. Rev. D* **78** (2008) 074006.
  - [18] F. Bruckmann, C. Gattringer and C. Hagen, private communication.
  - [19] Y. Aoki *et al.*, arXiv:0903.4155 [hep-lat].
  - [20] A. Bazavov *et al.*, arXiv:0903.4379 [hep-lat].